

Time-resolved dynamics of electron wave packets in chaotic and regular quantum billiards with leads

I. V. Zozoulenko,^{1,2,*} and T. Blomquist^{2,†}¹*Department of Science and Technology (ITN), Linköping University, S-60174 Norrköping, Sweden*²*Department of Physics (IFM), Linköping University, S-58183 Linköping, Sweden*

(Received 1 November 2002; revised manuscript received 3 December 2002; published 28 February 2003)

We perform numerical studies of wave packet propagation through open quantum billiards whose classical counterparts exhibit regular and chaotic dynamics. We show that for $t \lesssim \tau_H$ (τ_H being the Heisenberg time), the features in the transmitted and reflected currents are directly related to specific classical trajectories connecting the billiard leads. When $t \gtrsim \tau_H$, the calculated quantum-mechanical current starts to deviate from its classical counterpart, with the decay rate obeying a power law that depends on the number of decay channels. In a striking contrast to the classical escape from chaotic and regular systems (exponentially fast $e^{-\gamma t}$ for the former versus power-law $t^{-\xi}$ for the latter), the asymptotic decay of the corresponding quantum systems does not show a qualitative difference.

DOI: 10.1103/PhysRevB.67.085320

PACS number(s): 73.23.Ad, 05.45.Mt, 89.75.Da

I. INTRODUCTION

Low-dimensional nanometer-scaled semiconductor structures, quantum dots (sometimes called quantum electron billiards), represent artificial man-made systems which are well suited for the study of different aspects of quantum-mechanical scattering.¹ The conductance of quantum dots as a function of external parameter (magnetic field, Fermi energy, shape distortion, etc.) exhibits seemingly random but reproducible fluctuations originating from the interference of coherent electron waves inside the dot. The majority of studies of electron transport in such systems have focused mainly on the stationary electron dynamics. In recent years, however, interest in the temporal aspect of quantum scattering has gained prominence.^{2,3} This includes, e.g., studies of the ac admittance of mesoscopic capacitors,⁴ time delay distributions,⁵ correlation decay in quantum billiards and related systems,⁶ and others.

Furthermore, many core starting points in the description of stationary scattering in quantum dots rely heavily on the properties of the system in the time domain. In particular, the semiclassical approach exploits the difference between the classical escape rate from the cavities with chaotic and regular (or mixed) dynamics (exponentially fast $e^{-\gamma t}$ for the former versus power-law $t^{-\xi}$ for the latter⁷). This difference in the classical dynamics translates into the difference in observed transport properties (statistics of the fluctuations,^{8,9} a shape of the weak localization,¹⁰ fractality of the conductance oscillations,¹¹ etc.).

On the other hand, for chaotic cavities, quantum-mechanical approaches predict the qualitatively different, universal power-law escape rate,^{12,13}

$$dP(t)/dt \sim t^{-\beta M/2-1}, \quad (1)$$

where $P(t)$ is the survival probability, M is the number of decay channels, and $\beta=1$ (2) for the system with (without) time-reversal invariance. Note that the specific power of the decay law (1) depends on the initial population of the states as well as on the strength of the coupling.^{5,13} The origin of

the power-law decay can easily be understood with the help of heuristic arguments based on an averaging over the exponential decays of many individual states that mediate the transport through the billiard.¹³ The nonexponential decay of a quantum system with chaotic classical dynamics has been indirectly demonstrated¹⁴ in a weakly coupled microwave stadium billiard. Note that the problem of the escape of a quantum particle from a chaotic cavity is conceptually similar to the asymptotic behavior of the current relaxation time in disordered conductors attached to ideal metallic leads.¹⁵ In the latter case the asymptotic behavior of the corresponding distribution deviates strongly from the corresponding classical decay, with the averaged conductance decreasing more slowly than any exponential function. This behavior is due to the existence of nearly localized states that can trap electrons for a long time.

The quantum-mechanical power-law decay time for the chaotic cavity is expected to deviate from the semiclassical (SC) decay at a crossover time t_{cross} , which is of the order of the Heisenberg time $\tau_H = \hbar/\Delta$, Δ being the mean level spacing of the cavity.¹² Note that τ_H also defines the quantum relaxation time scale for the case of disordered conductors.¹⁵

Let us now estimate the Heisenberg time τ_H for the system at hand. The main focus of the present study is the ballistic semiconductor quantum dots in a regime typically accessible in an experiment. A typical size of the dot is in the range of $L=0.5-2 \mu\text{m}$; the dot is connected to electron reservoirs by means of two quantum point contacts (leads) typically supporting $\alpha=1-5$ propagating modes, and the Fermi wavelength of electrons is $\lambda \sim 50 \text{ nm}$. With this range of parameters we are in a semiclassical regime ($L/\lambda \gg 1$) as far as the electron dynamics in the dot is concerned. However, because the number of modes α is rather small, the coupling to the environment has a wave nature and cannot be treated semiclassically (i.e., the diffractive effects in the leads are expected to play a role). Note that the majority of studies on microwave billiards fall in the same region of parameters α and L/λ (Ref. 16).

Expressing the Heisenberg time $\tau_H = m^* L^2 / 2\pi\hbar$ in units of the traversal time $t_{tr} = L/v_F$ (m^* is the effective mass and v_F is the Fermi velocity), we get a simple estimate $\tau_H/t_{tr} = L/\lambda$. We thus conclude that the characteristic time scale during which the quantum-mechanical decay is expected to take over the classical one in a typical quantum dot ($L = 1 \mu\text{m}$, $\lambda \sim 50 \text{ nm}$) corresponds to $\tau_H/t_{tr} \approx 20$ classical bounces in the billiard. At the same time, the numerical calculations show that the difference between the classical decay of chaotic and regular-mixed cavities might become discernible only after ~ 20 – 50 bounces—that is, on times that are comparable or even exceed τ_H (see below, Sec. III).

Nevertheless, the semiclassical predictions (essentially based on the classical escape asymptotics) are widely used in experiment to distinguish between the chaotic and regular-mixed dynamics in quantum billiards.¹ Is it thus possible to reconcile the semiclassical and quantum mechanical approaches, or should some of the semiclassical predictions be used with a certain caution or even be revised? Another related question is whether the quantum-mechanical decay is different for chaotic and regular quantum billiards. [Note that the quantum-mechanical decay, Eq. (1), is obtained for the case of chaotic dynamics.] In other words, does the long-time decay asymptotics of the *quantum* systems reflect the underlying *classical* dynamics (chaotic or regular)? Motivated by these questions we present here results of direct quantum-mechanical calculations of the passage and escape of electron wave packets in two-dimensional electron billiards.

Note that quantum relaxation in open chaotic systems has been studied in Ref. 17. It was shown there that the quantum dynamics of open chaotic systems follows the classical decay behavior only up to a new quantum relaxation time scale $t_q = \tau_H / (T\sqrt{M})$, where T is the strength of coupling and M is the number of decay channels. When the number of channels $M \rightarrow \infty$, the new quantum scale t_q is much shorter than the Heisenberg time τ_H . This behavior has been verified for a model system of the quantum kicked rotator with absorption. In the cases of the two-terminal semiconductor quantum dots studied here, the number of decay channels $M = 2\alpha$, where $\alpha = 1$ – 5 and $T = 1$. Therefore, the new quantum relaxation time is of the order of the Heisenberg time $t_q = \tau_H / \sqrt{M} \sim \tau_H$ and we do not expect to see a clear manifestation of the new hierarchy of the characteristic time scales for the system at hand. Results of our numerical simulations confirm this expectation. In fact, the classical features persist in the quantum current even for times somewhat larger than τ_H ; see below, Sec. III. It is also important to note that the results of Ref. 17 focus on the time frame $t \ll \tau_H$. In contrast, in the present study we are interested in both characteristic time frames $t < \tau_H$ and $t > \tau_H$, and we focus on the crossover to the quantum power-law decay which takes place at $t_{cross} \sim \tau_H$.

To the best of our knowledge, all of the studies of wave packets dynamics in *open* systems presented so far have mostly been restricted to (a) a quantum limit where the characteristic size of the system L was of the order of the average wavelength of the wave packet $\langle \lambda \rangle$ and (b) to an initial stage

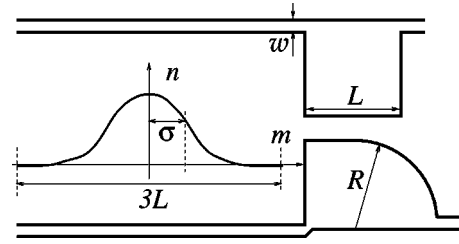


FIG. 1. A square and a quarter-stadium shaped billiard connected to semi-infinite leads; $L = R, L/w = 8$. The half-width of the wave packet $\sigma = 0.4L$; at $t = 0$ the wave packet is distinct from zero in the interval of $3L$. The average wavelength of the wave packet $\langle \lambda \rangle = 2\pi/\langle k \rangle = 0.8w$.

of the wave packet evolution $t \lesssim 1$ (t is in units of the traversal time). The time-dependent solution of the Schrödinger equation was typically obtained on the basis of direct schemes approximating the exponential time propagator.¹⁸ With such methods the task of tracing the long-time evolution of a wave packet in a realistic quantum dot would be forbiddingly expensive in terms of both computing power and memory. In the present paper we therefore implement a spectral method based on the Green function technique,¹⁹ which allows us to (a) reach a semiclassical regime $\langle \lambda \rangle \gg L$ and (b) approach a long-time asymptotics $t \gg 1$ corresponding to 10^4 – 10^5 bounces of a classical particle in a billiard.

The paper is organized as follows. A brief discussion of the computational method is given in Sec. II. The results of numerical simulations for two representative billiards (a regular square and a chaotic stadium) are presented in Sec. III. We provide a detailed discussion of our findings for two different regimes, initial decay $t < \tau_H$ (Sec. III A) and long-time asymptotics $t > \tau_H$ (Sec. III B). Our main conclusions are summarized in Sec. IV.

II. METHOD OF CALCULATIONS

We have studied the temporal evolution of wave packets in square, Sinai, and stadium billiards of various shapes. As all of these exhibit similar features we only present here results for two representative geometries, a square (which is classically regular) and a quarter-stadium (which is classically chaotic); see Fig. 1. The billiards are connected to two semi-infinite leads that can support one or more propagating modes. Magnetic field is restricted to zero. We assume a hard wall confinement both in the leads and in the interior of billiards.

The dynamics of the wave packet is governed by the time-dependent Schrödinger equation

$$\left(i\hbar \frac{\partial}{\partial t} - H \right) |\psi(t)\rangle = 0, \quad (2)$$

where H is the Hamiltonian operator and $|\psi(t)\rangle$ is the wave function. To study the time evolution of the initial state we follow Stóvneng and Hauge¹⁹ and perform the Laplace transform of Eq. (2), $|\tilde{\psi}(s)\rangle = \mathcal{L}|\psi(t)\rangle$, followed by an integration by parts,

$$|\tilde{\psi}(s)\rangle = \frac{i\hbar}{i\hbar s - \hat{H}} |\psi(0)\rangle.$$

Performing the inverse Laplace transform and changing variables in the Mellin inversion integral $i\hbar s \rightarrow z$ we obtain

$$|\psi(t)\rangle = \frac{i}{2\pi} \int_{-\infty+i0}^{\infty+i0} dz \hat{G}(z) |\psi(0)\rangle e^{-izt/\hbar}, \quad (3)$$

where we have introduced the Green function operator $\hat{G} = (z - \hat{H})^{-1}$, and taken into account the fact that all the poles of the Green function lie in the lower z plane. With the help of Eq. (3), the calculation of the temporal evolution of the initial state is effectively reduced to the computation of the Green function of the Hamiltonian operator \hat{H} in the energy domain.

In order to perform numerical calculations we discretize the system and introduce a standard tight-binding lattice Hamiltonian

$$\hat{H} = \sum_{m,n} [|m,n\rangle (\epsilon_0 + V_{nm}) \langle m,n| - u \{ |m,n\rangle \langle m,n+1| + |m,n\rangle \langle m+1,n| + \text{H.c.} \}], \quad (4)$$

where u is the nearest-neighbor hopping amplitude, ϵ_0 is the lattice site electron energy, and V_{nm} is the potential energy. The matrix element $\langle m,n|\psi\rangle$ defines the probability amplitude of finding the electron on the site (m,n) , with $m=ax$, $n=ay$, and a being the lattice constant; x and y are the longitudinal and transverse coordinates, respectively. In our calculations we always choose a small enough such that $ka \ll 1$, k being the wave vector. In this limit the tight-binding Hamiltonian (4) yields the familiar Schrödinger equation, provided $\epsilon_0 = 4u$ and $u = \hbar^2/2m^*a^2$, with m^* the effective mass.

Let us consider a minimum-uncertainty wave packet of average energy E which enters a billiard from the left lead in one of the transverse modes α . We can then write the initial state in the left lead at $t=0$ in the form

$$|\psi_\alpha(0)\rangle = \sum_{mn} \phi_m^\alpha f_n^\alpha |mn\rangle, \quad (5)$$

$$\phi_m^\alpha = \frac{1}{(2\pi)^{1/4} \sqrt{\sigma}} e^{-(m-m_0)^2/4\sigma^2 + ik_\parallel^\alpha m}, \quad (6)$$

where $f_n^\alpha = \sqrt{2/w} \sin(\pi an/w)$ is the eigenfunction of the transverse motion, and w is the width of the leads (measured in units of a lattice constant a). $\langle k \rangle = 2\pi/\langle \lambda \rangle = \sqrt{E/u}$ is the average wave number (in units of a^{-1}), where $u = \hbar^2/2m^*a^2$ and m^* being the effective mass. Furthermore, $\langle k \rangle^2 = k_\parallel^{\alpha 2} + k_\perp^{\alpha 2}$, $k_\perp^\alpha = \pi\alpha/w$, where k_\parallel^α and k_\perp^α are the longitudinal and transverse wave vectors, respectively. After the wave packet enters the billiard, it will leak out through both of the leads in all the available modes β . For computational purposes it is convenient to pass from real space to the mixed-space-mode representation of the state vector $|\psi\rangle$ ac-

ording to $|m,\alpha\rangle = \sum_n f_n^\alpha |mn\rangle$. The wave function in, e.g., the right lead can then be written in the form

$$|\psi_\alpha(t)\rangle = \sum_{m\beta} c_{\beta\alpha}^m(t) |m\beta\rangle, \quad (7)$$

where $c_{\beta\alpha}^m$ gives the probability of finding a particle in the slice m in the transverse mode β , provided the initial state enters the billiard in the mode α . Discretizing the standard expression for the quantum-mechanical current, $j(x,y) = i\hbar/2m^*(\psi\nabla\psi^* - \psi^*\nabla\psi)$, we obtain, using Eq. (7), the following expression for the total current $J = \int dy j(x,y)$ through the slice m in the leads expressed via coefficients $c_{\beta\alpha}^m(t)$:

$$J = \frac{i\hbar}{m^*a} \sum_{\beta} [c_{\beta\alpha}^m (c_{\beta\alpha}^{m+1*} - c_{\beta\alpha}^{m-1*}) - \text{c.c.}]. \quad (8)$$

We calculate the coefficients $c_{\beta\alpha}^{m+1}$ in Eq. (8) by computing a matrix element $\langle m\beta|\psi\rangle$ using Eqs. (3)–(7):

$$c_{\beta\alpha}^m(t) = \frac{i}{2\pi} \int_{-\infty+i0}^{\infty+i0} dz \sum_{m'} G_{\beta\alpha}^{mm'}(z) \phi_m^\alpha e^{-izt/\hbar}, \quad (9)$$

where $G_{\beta\alpha}^{mm'}(z)$ stands for the matrix element $\langle m\beta|G(z)|m'\alpha\rangle$ of the Green function of the whole system (billiard and semi-infinite leads). We compute the matrix elements of the Green function by making use of the modified recursive Green-function technique described in detail in Ref. 20.

Note that the quantum-mechanical current is related to the survival probability in the billiard, Eq. (1), by the obvious relation

$$dP(t)/dt = -J_l(t) - J_r(t), \quad (10)$$

where $J_l(t)$ and $J_r(t)$ stand for the currents flowing into the left and right leads, respectively. Note also that the function $J_l(t) + J_r(t)$ can be interpreted as the distribution of the time delays in the billiard.⁵

Special care has been taken to ensure the reliability of the results of the numerical simulations. In particular, this includes a thorough control of the conservation of the total current. We have also calculated the temporal evolution of the wave packet in the infinite wire of width w and found excellent agreement with the analytical results for the case of a one-dimensional (1D) lattice.¹⁹ Finally, the method we have developed correctly reproduces the conductance quantization of the quantum point contact.

III. RESULTS AND DISCUSSION

A. Initial decay ($t \lesssim \tau_H$)

Let us first concentrate on the initial phase of the wave packet dynamics. Our choice of parameters describing the wave packet, σ and $\langle k \rangle$, ensures that the spreading of the wave packet becomes noticeable only after relatively long time $t \gtrsim 50$ [here and hereafter we measure time in units of the traversal time $t_{tr} = L/\langle v \rangle$, $\langle v \rangle = L/(\hbar\langle k \rangle/m^*)$; the cur-

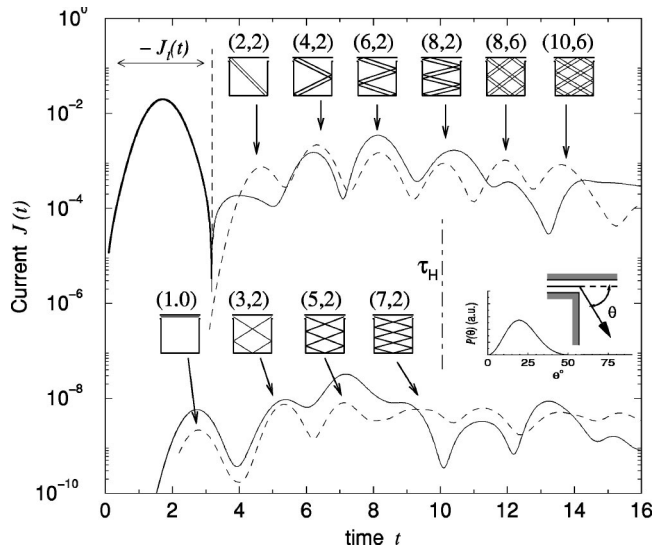


FIG. 2. Quantum-mechanical reflected and transmitted current through a square billiard (upper and lower solid curves, respectively). Dashed lines indicate corresponding *classical* currents. The wave packet enters the billiard in the second mode $\alpha=2$; $\langle k \rangle = 2.5w/\pi$. The insets show classical reflected and transmitted trajectories; the numbers in the parentheses are the so-called winding numbers indicating how many times an electron traverses the billiard in the longitudinal and transverse directions. The inset to the right shows an angular distribution of injected electrons $P(\theta)$ calculated in the Fraunhofer approximation for $\alpha=2$. The Heisenberg time τ_H is indicated by a dot-dashed line. The curves are shifted for clarity.

rent is measured in units of $\hbar/2m^*a$]. The width of the wave packet in the k space is of the order $\Delta k \sim 1/w$. This allows us to launch a wave packet propagating in one specified mode in the leads (for the hard wall confinement the distance between consecutive transverse modes in the leads is given by π/w).

Figure 2 shows the quantum-mechanical current for the square billiard in the time interval $t \lesssim 15$. The initial period of time $0 < t \lesssim 3$, when the current through the left lead $J_l(t)$ is negative, corresponds to a buildup phase when the wave packet enters the billiard. Having entered the billiard, the wave packet starts to leak out through the leads and the calculated quantum-mechanical currents J_l, J_r show a series of pronounced peaks. To outline the origin of these peaks we calculate the leakage current of a corresponding *classical* wave packet in the same billiard. In the classical calculations we take into account the diffractive effects in the leads in the framework of the standard Fraunhofer diffraction approximation by injecting the electrons with the corresponding angular distribution $P(\theta)$ (the inset in Fig. 2 shows a calculated angular probability distribution for the lead geometry under consideration). The very good correspondence between the quantum-mechanical and classical results allows us to ascribe each peak in the *quantum-mechanical* transmitted-reflected currents to a specific *classical* trajectory connecting the billiard leads; see the insets in Fig. 2.

The relative height of each peak depends on the density of the corresponding trajectories and on the angular distribution

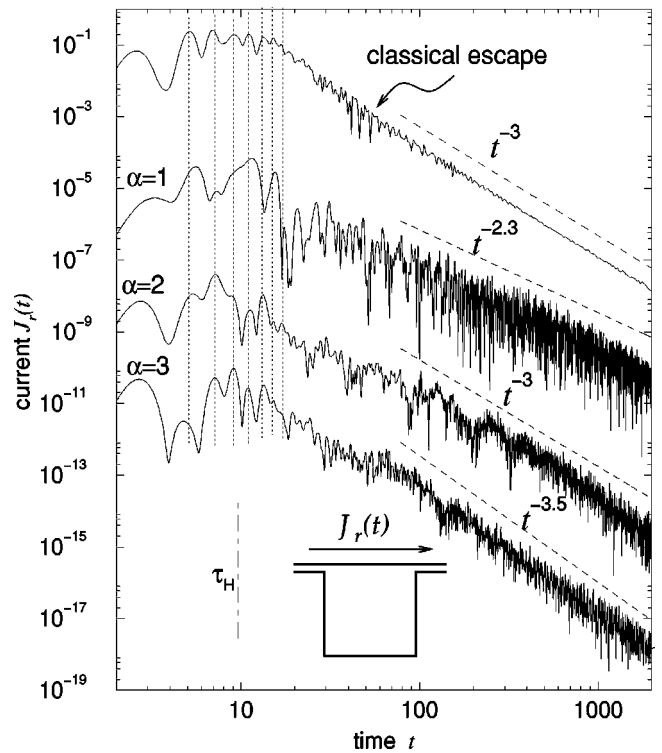


FIG. 3. Quantum-mechanical transmitted current through a square billiard for different incoming modes of the wave packet, $\alpha=1,2,3$, with $\langle k \rangle \pi/w = 1.5, 2.5, 3.5$, respectively. The upper curve indicates corresponding *classical* current. Vertical dotted lines are guides for an eye indicating the same positions of the peaks in the current. Dashed lines give the asymptotic power-law decay obtained by the best fit in the interval $80 < t < 2000$. The Heisenberg time τ_H is indicated by a dot-dashed line. The curves are shifted for clarity.

for a given incoming mode α . The effect of the latter is clearly seen in Fig. 3, where the quantum-mechanical current in a square billiard is shown for three different incoming modes of the wave packet, $\alpha=1,2,3$. At the initial stage of the current decay, $t \lesssim 20$, the positions of the peaks are the same for all incoming modes, although their absolute values differ. This is explained by the fact that the angular distribution $P(\theta)$ is different for different α , with its maximum being shifted to larger θ for higher modes α . We conclude this discussion by pointing out that all quantum billiards studied here exhibit similar characteristic peaks in the current at $t \lesssim \tau_H$ which can be explained in terms of corresponding classical trajectories (see, e.g., Fig. 4, where the calculated quantum-mechanical and classical currents in a stadium-shaped billiard show the same features for $t \lesssim \tau_H$).

B. Long-time asymptotics ($t \gtrsim \tau_H$)

Let us now focus on the long-time asymptotics of the wave packet dynamics. As discussed in the Introduction, we expect that the quantum-mechanical dynamics starts to deviate from its classical counterpart at time $t_{cross} \sim \tau_H$. The numerical calculations confirm this expectation. Consider the square billiard; see Fig. 3. Its classical escape rate is independent of the number of modes in the leads and is well

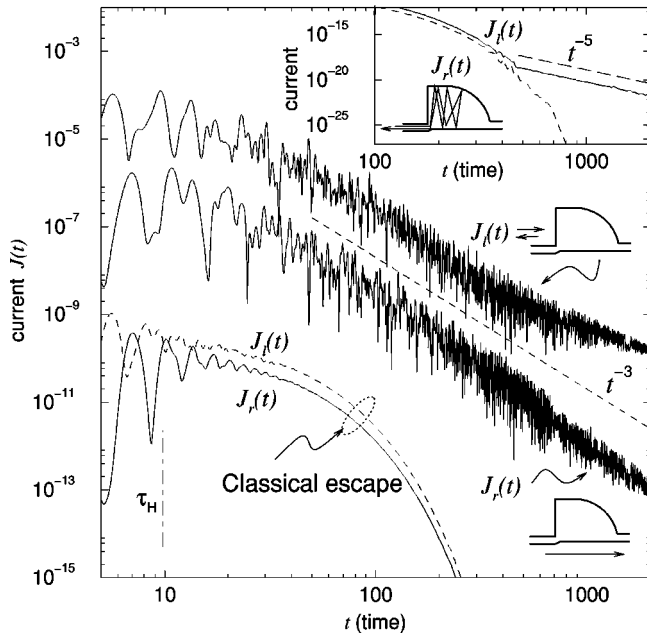


FIG. 4. Quantum-mechanical reflected and transmitted current through a stadium-shaped billiard. Lower curves show corresponding *classical* currents. The wave packet enters the billiard in the second mode $\alpha = 2$; $\langle k \rangle = 2.5w/\pi$. The inset shows a long-time asymptotic of classical escape along with the example of a bouncing-ball trajectory. Dashed lines give the asymptotic power-law decay obtained by the best fit in the interval $50 < t < 2000$. The Heisenberg time τ_H is indicated by a dot-dashed line. Time is measured in the units of the traversal time of the equivalent square of the same area. The curves are shifted for clarity.

approximated by a power law $\sim t^{-3}$. Comparison with the quantum-mechanical escape shows that classical trajectories can still be traced in the quantum current even for the times somehow larger than τ_H .

However, at the time scale $t \gtrsim 2\tau_H$ the identification of the characteristic peaks in the quantum-mechanical current is no longer possible and the quantum-mechanical decay shows qualitative new features. In particular, the calculated quantum-mechanical decay depends on the number of modes in the leads and follows the power-law decay with the exponents $\xi = 2.3, 3, 3.5$ for modes $\alpha = 1, 2, 3$ correspondingly. These values are somehow different from those expected from Eq. (1), $\xi = 2, 3, 4$. (In a billiard with two leads a number of decay channels is given by $M = 2\alpha$.)

One of the reasons for the above discrepancy may be related to the fact that in a billiard system the details of the coupling between the leads can be important for the selection of particular states that mediate transport through the system. Furthermore, in the case of open cavities (i.e., strong coupling), the broadening of some resonant states has essentially non-Lorentzian character²¹ [on the contrary, Eq. (1) corresponds to the case when all resonant states are excited with the same probability at $t=0$ and have the Lorentzian line shape]. It is also worth to mention that Eq. (1) is based on the random matrix theory and similar stochastic approaches.^{5,12,13} The predictions of these theories tend to be rather general in nature, and they usually fail to account for

specific features of the geometry under consideration (such as details of the lead position, existence of periodic orbits, etc.).

Let us now discuss the wave-packet evolution in a stadium-shaped billiard. Classically, this billiard exhibits chaotic dynamics, and its classical long-time escape shows fast exponential decay; see Fig. 4. The corresponding long-time quantum-mechanical decay for such a system is, however, qualitatively different. The difference between the classical and quantum-mechanical escapes becomes clearly discernible at the same time scale as for the square. Namely, when $t \gtrsim 2\tau_H$ it is no longer possible to provide a reliable identification of the peaks in the quantum-mechanical current in terms of classical trajectories. At this time scale the quantum-mechanical escape starts to follow a power law similar to the one observed for the square. In this respect it should be noted that for the quantum billiards studied here the initial stage of evolution including the crossover region $t_{cross} \sim \tau_H$ is dominated by the pronounced peaks related to the geometry-specific classical trajectories. Therefore, without an ensemble averaging it is rather difficult to indicate an exact value of time when a crossover to a quantum decay takes place for a billiard of a given geometry. Therefore, our estimation of the crossover time $t_{cross} \sim \tau_H$ necessarily includes some uncertainty, typically of the range of ~ 10 bounces.

The long-time asymptotics of the quantum decay of a classically chaotic stadium follows the similar power-law dependence as for the classically regular square. This is in striking contrast to the corresponding classical decay (exponentially fast for chaotic versus power law for regular systems). This makes us conclude that quantum mechanics smears out the difference between classical chaotic and regular motion.

Note that the billiard at hand is designed in such a way that the classical escape through the left lead changes its asymptotics from the exponential one to a slower power-law decay at $t \sim 500$. This behavior is caused by bouncing-ball orbits²² which are accessible via the left lead only (see the inset in Fig. 4). It is interesting to note that the corresponding quantum-mechanical current through the left lead also starts to show slower decay at $t \sim 500$ in comparison to the right lead. We therefore speculate that, even though the long-time asymptotics of the quantum-mechanical and classical decays are qualitatively different, the quantum-mechanical decay still reflects some features of the underlying classical dynamics.

Finally, we point out some possible implications of the obtained results for the interpretation of experimental data. As stressed in the Introduction, the difference in the *classical* decay rate in chaotic, regular, or mixed systems is often used in various semiclassical approaches to describe observed transport properties of the quantum systems (statistics of the fluctuations, the shape of weak localization, fractal conductance fluctuations, etc.).^{1,8-11} However, an inspection of the *classical* decay in regular and chaotic billiards (Figs. 3 and 4; see also Ref. 23) demonstrates that corresponding asymptotics (power law for the former and exponential decay for the latter) becomes clearly discernible only after $t_{class} = 20-50$

bounces in the billiard. (Initial stages of the evolution $t \lesssim t_{class}$, regardless of the character of the electron dynamics, are dominated by the pronounced geometry-specific features related to the specific trajectories characteristic for a given shape). At the same time, our numerical findings demonstrate that the crossover to the quantum-mechanical power-law decay occurs on the time scale of the order of the Heisenberg time τ_H . In a typical quantum dot τ_H is comparable (and can even be smaller) than the above-mentioned time scale t_{class} , when the difference between *classical regular and chaotic systems* becomes discernible. Our findings thus strongly indicate that application of some of the semiclassical predictions (essentially based on the classical escape asymptotics) might not always be justified because the quantum relaxation can occur on a time scale t_{cross} smaller than t_{class} . Note that different aspects of applicability of semiclassical approaches to quantum dot systems have been discussed in Refs. 23 and 24.

IV. CONCLUSIONS

We study temporal dynamics of electron escape in chaotic and regular quantum dots in regimes typically accessible in the experiment. We find that during the initial phase, $t \lesssim \tau_H$ (τ_H being the Heisenberg time), the quantum-mechanical decay closely follows the classical one, so that all features in the quantum-mechanical current leaking out of the billiard can be explained in terms of geometry-specific classical trajectories between the leads.

The time scale $t_{cross} \sim \tau_H$ determines the crossover to quantum-mechanical decay. When $t \gtrsim \tau_H$, the calculated quantum-mechanical current starts to deviate from its classi-

cal counterpart, with the decay rate obeying a power law that depends on the number of decay channels. The exponents obtained were somehow different from those expected from Eq. (1); we provide possible explanations for this discrepancy. In striking contrast to the classical escape from chaotic and regular systems (exponentially fast $e^{-\gamma t}$ for the former versus power-law $t^{-\xi}$ for the latter), the asymptotic decay of the corresponding quantum systems does not show a qualitative difference. This makes us conclude that quantum mechanics smears out the difference between classical chaotic and regular dynamics.

We also discuss possible implications of the obtained results for the interpretation of the experimental data. In particular, our findings strongly indicate that application of some of the semiclassical predictions (essentially based on the classical escape asymptotics) might not always be justified because the crossover to the power-law *quantum decay* can occur at the time scale t_{cross} shorter than t_{class} , the time when the *classical escape asymptotics* becomes clearly different for chaotic and regular systems.

Finally, the results reported in the present paper can be directly tested experimentally in the variety of systems including semiconductor quantum dots,¹ microwave cavities,^{16,25} acoustical,²⁶ and optical billiards.²⁷

ACKNOWLEDGMENTS

Financial support of Vetenskapsrådet (I.V.Z.) and the National Graduate School of Scientific Computing (T.B.) is greatly acknowledged. Discussions with M. Büttiker are greatly appreciated.

*Electronic address: igozo@itn.liu.se

†Electronic address: torbl@ifm.liu.se

¹C. M. Marcus, A. J. Rimberg, R. M. Westervelt, P. F. Hopkins, and A. C. Gossart, Phys. Rev. Lett. **69**, 506 (1992); A. S. Sachrajda, R. Ketzmerick, C. Gould, Y. Feng, P. J. Kelly, A. Delage, and Z. Wasilewski, *ibid.* **80**, 1948 (1998).

²S. Tomsovic and E. J. Heller, Phys. Rev. Lett. **67**, 664 (1991).

³M. Büttiker, J. Low Temp. Phys. **118**, 519 (2000).

⁴V. A. Gopar, P. A. Mello, and M. Büttiker, Phys. Rev. Lett. **77**, 3005 (1996).

⁵Y. V. Fyodorov and H.-J. Sommers, J. Math. Phys. **38**, 1918 (1997).

⁶P. W. Brouwer, K. M. Frahm, and C. W. J. Beenakker, Phys. Rev. Lett. **78**, 4737 (1997).

⁷W. Bauer and G. F. Bertsch, Phys. Rev. Lett. **65**, 2213 (1990).

⁸R. Blümel and U. Smilansky, Phys. Rev. Lett. **60**, 477 (1988).

⁹R. A. Jalabert, H. U. Baranger, and A. D. Stone, Phys. Rev. Lett. **65**, 2442 (1990).

¹⁰H. U. Baranger, R. A. Jalabert, and A. D. Stone, Phys. Rev. Lett. **70**, 3876 (1993).

¹¹R. Ketzmerik, Phys. Rev. B **54**, 10 841 (1996).

¹²C. H. Lewenkopf and H. A. Weidenmüller, Ann. Phys. (N.Y.) **212**, 53 (1991).

¹³F.-M. Dittes, H. L. Harney, and A. Müller, Phys. Rev. A **45**, 701 (1992); H. L. Harney, F.-M. Dittes, and A. Müller, Ann. Phys. (N.Y.) **220**, 159 (1992).

¹⁴H. Alt, H.-D. Gräf, H. L. Harney, R. Hofferberg, H. Lengeler, A. Richter, P. Schardt, and H. A. Weidenmüller, Phys. Rev. Lett. **74**, 62 (1995).

¹⁵B. L. Altshuler, V. E. Kravtsov, and I. V. Lerner, Pis'ma Zh. Éksp. Teor. Fiz. **45**, 160 (1987) [JETP Lett. **45**, 199 (1987)]; B. A. Muzykantskii and D. E. Khmel'nitskii, Phys. Rev. B **51**, 5480 (1995); I. E. Smolyarenko and B. L. Altshuler, *ibid.* **55**, 10 451 (1997).

¹⁶U. Kuhl, E. Persson, M. Barth, and H.-J. Stöckmann, Eur. Phys. J. B **17**, 253 (2000); T. Blomquist, H. Schanze, I. V. Zozoulenko, and H.-J. Stöckmann, Phys. Rev. E **66**, 026217 (2002).

¹⁷G. Casati, G. Maspero, and D. L. Shepelyansky, Phys. Rev. E **56**, R6233 (1997); K. M. Frahm, *ibid.* **56**, R6237 (1997); D. V. Savin and V. V. Sokolov, *ibid.* **56**, R4911 (1997).

¹⁸T. Palm, J. Appl. Phys. **74**, 3551 (1993); J. B. Wang and S. Midgley, Phys. Rev. B **60**, 13 668 (1999).

¹⁹J. A. Stóvneng and E. H. Hauge, Phys. Rev. B **44**, 13 582 (1991).

²⁰I. V. Zozoulenko, F. A. Maaß, and E. H. Hauge, Phys. Rev. B **53**, 7975 (1996); **53**, 7987 (1996).

²¹I. V. Zozoulenko, R. Schuster, K.-F. Berggren, and K. Ensslin, Phys. Rev. B **55**, R10 209 (1997); I. V. Zozoulenko and K.-F. Berggren, *ibid.* **56**, 6931 (1997).

²²H. Alt, H.-D. Gräf, H. L. Harney, R. Hofferberg, H. Rehfeld, A. Richter, and P. Schardt, Phys. Rev. E **53**, 2217 (1996).

- ²³T. Blomquist and I. V. Zozoulenko, Phys. Rev. B **64**, 195301 (2001).
- ²⁴L. Wirtz, J.-Z. Tang, and J. Burgdörfer, Phys. Rev. B **59**, 2956 (1999).
- ²⁵J. Stein, H.-J. Stöckmann, and U. Stoffregen, Phys. Rev. Lett. **75**, 53 (1995).
- ²⁶J. de Rosny, A. Tourin, and M. Fink, Phys. Rev. Lett. **84**, 1693 (2000).
- ²⁷N. Friedman, A. Kaplan, D. Carasso, and N. Davidson, Phys. Rev. Lett. **86**, 1518 (2001); V. Milner, J. L. Hanssen, W. C. Campbell, and M. G. Raizen, *ibid.* **86**, 1514 (2001).